Brightness enhancement on random-distributed-feedback Raman fiber lasers pumped by multimode diodes

Xiulu Hao [1], Chenchen Fan [1], Yang Li [1], Zhiyong Pan [1,2], Jinyong Leng [1,2], Tianfu Yao [1,2*], Bing Lei [1], and Pu Zhou [1*]

[1]College of Advanced Interdisciplinary Studies, National University of Defense Technology, Changsha 410073, China
2Nanhu Laser Laboratory, National University of Defense Technology, Changsha 410073, China

*Correspondence to: Tianfu Yao and Pu Zhou, College of Advanced Interdisciplinary Studies, National University of Defense Technology, Changsha 410073, China. Email: yaotianfumary@163.com (T. Yao), zhoupu203@163.com (P. Zhou)

Abstract
The power scaling on short wavelengths (SWs) fiber lasers operating around 1 μm are in significant demand for applications in energy, environment, and industry. The challenge for performance scalability of high-power SW lasers based on rare-earth (RE) doped fiber primarily lies on the physical limitations, including reabsorption, amplified spontaneous emission (ASE), and parasitic laser oscillation. Here, we demonstrate an all-fiberized, purely passive SW (1018nm) random-distributed-feedback Raman fiber laser (RRFLs) to validate the capability of achieving high-power output at SWs based on direct pumping by multimode LDs. Directly pumped by multimode LDs, the high-brightness RRFLs delivered over 656 W, with an electro-optical efficiency of 20% relative to the power. The slope efficiency is 94%. The beam quality M^2 factor is 2.9 (which is ~20 of pump) at the maximum output signal power, achieving the highest brightness enhancement (BE) of 14.9 in RRFLs. To the best of our knowledge, this achievement also represents the highest power record of RRFLs utilizing multimode diodes for directly pumping. This work may not only provide a new insight into the realization of high-power, high-brightness RRFLs but also is a promising contender in the power scaling on SWs below 1 μm.

Keywords: fiber laser; purely passive gain; stimulated Raman scattering; random-distributed-feedback

10.1017/hpl.2024.8

I. INTRODUCTION

High-power short wavelengths (SWs) fiber lasers operating around 1 μm with high-brightness are highly required in many applications, such as material processing, nonlinear frequency conversion and spectral beam combining, etc. [1–4]. Meanwhile, due to the lower fractional thermal load as a result of the higher quantum efficiency, the thresholds of the transverse mode instability (TMI) [5-7] for the SWs fiber lasers based on ytterbium-doped fiber lasers (YDFL) are usually higher than those for the longer-wavelength fiber lasers operating around 1080 nm, which made the SWs fiber lasers promising for high-power systems [8,9]. However, due to the significantly higher levels of ASE induced by large signal absorption cross sections [10], high-power fiber laser systems operating at SWs around or below 1 μm [11] are found to be much more challenging compared to traditional wavelength band fiber lasers [12].

At present, most of the SWs output schemes are based on solid-state lasers such as laser diodes (LDs) [13]. One of the interesting possibilities is to directly pump purely passive fibers using available high-power multimode laser diodes (LDs) at 915–950 nm. This approach facilitates the generation of high-power Raman lasing within the wavelength range of 960–1020 nm, presenting a set of challenges for RE-doped fiber lasers [14]. 1018 nm is a commonly utilized special wavelength in YDFL, which is located near the 1μm band. Notably, this wavelength holds importance for tandem pumping of YDFL, as discussed in references [15-17, 20]. Study in this wavelength range can establish a robust experimental foundation for achieving higher power outputs in even shorter wavelength bands.

Currently, high-power 1018nm fiber lasers are primarily realized utilizing two main structures: amplifier-based [14-17] and oscillator-based configurations [18-25]. In the case of the 1018nm all-fiber master oscillator power amplifier (MOPA), studies in this area have been limited

https://doi.org/10.1017/hpl.2024.8 Published online by Cambridge University Press

due to the issue of reabsorption in the 1018nm wavelength range [15]. As a result, there have been limited reported achievements, with output powers reaching around 616W [17]. Compared to amplifiers, 1018nm oscillators have a simpler and more stable structure. While these studies show the potential of high-power oscillators, it is worth noting that the presence of resonator cavity structures in oscillators can lead to the occurrence of self-pulsing phenomena [26,27]. This phenomenon leads to the occurrence of nonlinear effects like Stimulated Raman Scattering (SRS) in high-power fiber laser systems [28,29]. Furthermore, the traditional structure based on RE-doped fiber oscillator is no longer suitable for SWs output, making it incapable of achieving higher laser output power. Therefore, it is crucial to explore new and innovative approaches for the development of SWs lasers.

As a novel fiber light source, random-distributed-feedback Raman fiber lasers (RRFLs) have attracted widespread attention due to its unique performance since they were initially introduced by Turitsyn et al. in 2010 [30-32]. In the past, limited by the brightness of LDs, researchers could only employ YDFL pumped by LDs to pump RRFLs, thereby achieving higher output power. However, the two-stage conversion for signal light through pumping results in a low electro-optical efficiency (less than 20%) of the laser system [13]. With the development of high-brightness LDs and high-nonlinear fiber technology, obtaining laser output based on direct pumping of passive fibers by LDs will be a new technological solution for achieving SWs laser in the future [33-36]. In 2018, Evmenova et. al demonstrated the first random lasing in the all-fiber scheme of directly pumped by laser diodes, with output power of 27 W and beam quality M^2 of 1.6 at 996 nm [33]. Although further power scaling is constrained by relatively poor pump brightness, the novel routine on wavelength expanding beyond general band of YDFL has been validated [34-37]. Therefore, RRFLs pumped by multimode diodes are attractive to achieve higher

https://doi.org/10.1017/hpl.2024.8 Published online by Cambridge University Press

power laser at SWs [34]. The combination of high-brightness multimode LDs and purely passive fibers will yield a notable "performance doubling" effect in generating SWs.

In this paper, we firstly demonstrate a half-open cavity all-fiberized SW (1018nm) RRFL directly pumped by multimode diodes, excluding any RE-dopant in the whole system. The potential on power scaling of SW RRFLs directly pumped by multimode LDs has been verified by the obtained output power of 656W. The slope efficiency is 94% and electro-optical conversion efficiency is ~20%. To the best of our knowledge, this result also represents the highest power record of RRFLs utilizing multimode LDs for direct pumping with SW output, showing great potential at power scaling at SWs below 1μm. We achieve a signal light output M^2 of 2.9(which is ~20 of pump), resulting in a BE of 14.9, the highest known BE in RRFLs to date. The findings and techniques explored in this study could pave the way for achieving high-power SWs laser output through multimode LDs direct pumping of passive fibers, providing a new insight into the realization of high-power, high-brightness RRFLs below 1 μm.

II. EXPERIMENTAL SETUP

The experimental setup for the purely passive RRFLs pumped by multimode LDs is depicted in Fig.1. Accordingly, the laser system in Fig.1 (a) follows a simple half-open cavity configuration and the LDs direct-pumped RRFLs significantly enhance system integration. The output of the pump system (as depicted in the illustration) is provided by a multimode diodes module with adjacent wavelengths, ranging from 954 nm to 986 nm, totaling 13 LDs with approximately 3 nm wavelength spacing. The laser from these LDs is coupled into the core of a commercial fiber using a Volume Bragg Grating (VBG). The core and cladding diameters of this fiber are 100 μm and 360μm, respectively, with a core numerical aperture (NA) of 0.22. The maximum output power of

https://doi.org/10.1017/hpl.2024.8 Published online by Cambridge University Press

the coupled pump is measured reaching to 1915 W with a coupling efficiency of 98%. The brightness[38,39] of the output multi-wavelength pump after spectral synthesis is about 6.7×10^{16} W/(m²·sr). The output spectrum of pump is measured at maximum output, as depicted in Fig.1 (b).

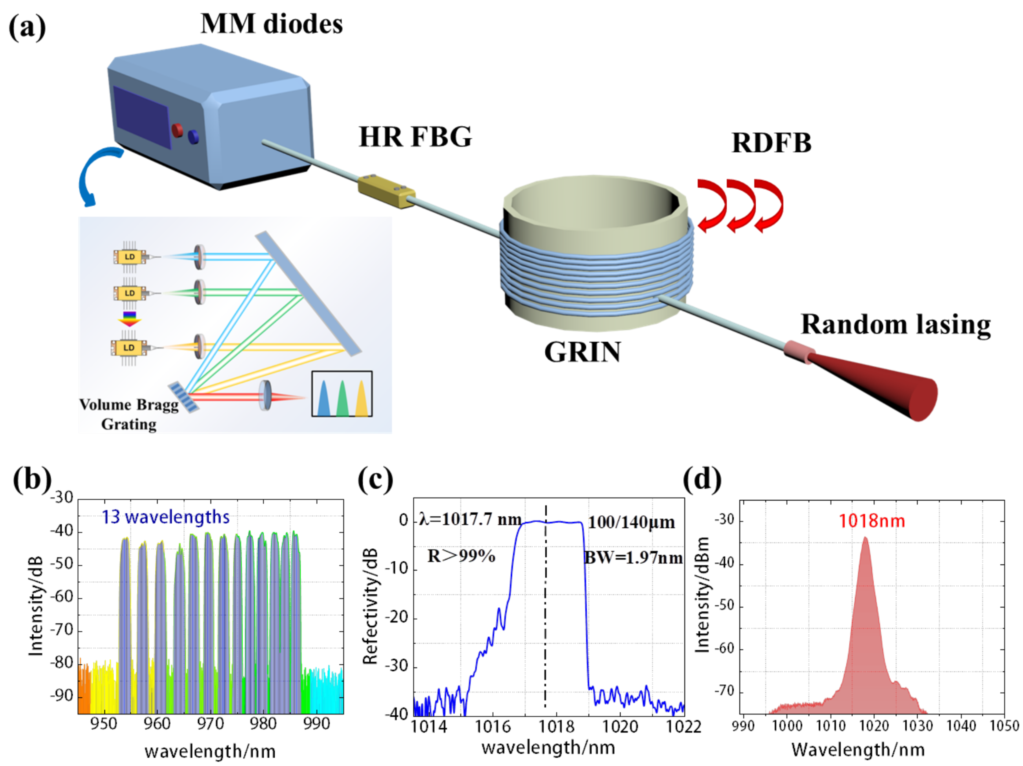

Figure 1. Random-distributed-feedback fiber lasers experimental setup. (a) Simplified RRFLs with LDs directly pumping. (b) The output spectrum of pump. (c) The reflection spectrum of the HR FBG. (d) The output spectrum of signal light. MM-LDs: multimode laser diodes; HR: highly reflective; GRIN: Graded-index; RDFB: Random Distributed Feedback.

The combined pump radiation is directed into a section of passive fiber with a 100/140μm core/cladding diameter with the fiber core NA of 0.25. After comparing the results obtained with various fiber lengths, it was concluded that an optimal fiber length of approximately 220m should be used. Further power scaling and conversion efficiency are limited by the power and brightness of LDs. Subsequently, it is introduced into a half-open cavity where a 1018nm high reflectivity fiber Bragg grating (HR FBG) and RDFB (Random Distributed Feedback) within a section of commercial purely passive multimode Graded-index (GRIN) fiber are present. The HR FBG, with

https://doi.org/10.1017/hpl.2024.8 Published online by Cambridge University Press

a reflectivity exceeding 99% at a center wavelength of 1017.7nm, exhibits a relatively narrow linewidth of 1.97nm at 3dB linewidth. The reflection spectrum of the HR FBG is shown in Fig. 1(c). The FBG with the mode-selection properties is UV-inscribed and has the same diameter and fiber core NA as the passive 100/140μm multimode GRIN fiber used. The transmission loss of the GRIN fiber is 1.5dB/km at 976nm. The output pigtailed fiber of the half-open cavity is spliced to a matched end cap (EC), which could avoid the damage to fiber end face. To characterize the output radiation, the collimated beam is split into the individual pump and signal beams by the dichroic mirrors (reflectivity＞99%@1018nm; transmissivity＞99%@954-986nm), whose power, spectrum, and beam quality parameter are measured respectively. For the signal laser, after filtering out the residual pump, the beam profiles and beam quality are examined using a charge-coupled device (CCD) camera and a beam quality monitor. Additionally, an oscilloscope is employed to capture the time-domain intensity data of the output beam. The output signal spectrum of the RRFLs is illustrated in Figure 1(d).

III. RESULTS AND DISCUSSIONS

Building upon this experimental configuration, we conducted an in-depth investigation of the output characteristics of a SW (1018nm) RRFL in the frequency, spatial, and temporal domains. This study aimed to gain a comprehensive understanding of its spatiotemporal dynamics, thereby providing a solid experimental foundation for future shorter wavelength system design [40,41].

A. The output characteristics of SW (1018nm) RRFL

Firstly, we analyzed and discussed the frequency spectrum output characteristics of the 1018nm RRFLs as a function of the signal light power. Figure 2 illustrates the influence of input pump power on the output signal characteristics. In Figure 2(a), the power spectrum of the filtered RRFLs

https://doi.org/10.1017/hpl.2024.8 Published online by Cambridge University Press

is depicted at different output powers. At a signal power of only 10W, higher-order Stokes light emerges at 1070nm and 1123nm. These wavelengths correspond to the second-order and third-order Raman shifts, respectively, and are close to the Raman gain peak of the silica-based fiber at around 13.2THz. As the signal power increases to 276W, the intensity of the higher-order Stokes light at these wavelengths weakens significantly. When the signal optical power exceeds 276W, the higher-order Stokes light disappears. The observed changes in the spectral characteristics are closely related to the distinctive half-open cavity structure of the random laser [32, 42, 43].

The cause of this behavior can be attributed to the process of cascaded stimulated Brillouin Scattering (SBS) [32]. In cavity-free Random Fiber Lasers, incident photons propagating through a long passive fiber a can be backscattered by the random refractive index, inhomogeneity induced weak Rayleigh scattering and amplified by the SRS. At the same time, the acoustic field generated by electrostriction induces moving, random density gratings, a process defined as Stimulated Brillouin Scattering (SBS) [42, 43]. Then, photons experiencing a frequency down-shift due to the Doppler Effect are excited by the transient temporal characteristics. The three insets with output power from 10W to 276W at the bottom present the output spectrum near the threshold, while another three insets at the top present the output spectrum well above the threshold. In the following section C, we will delve into a more detailed analysis by considering its temporal characteristics. To characterize the output radiation, the collimated beam is split into the individual pump and signal beams by the dichroic mirrors. With the increase in wavelength, the corresponding transmissivity also decreases, leading to that the residual pump at >975nm, >20 dB is higher than the residual pump at 955-965nm.

https://doi.org/10.1017/hpl.2024.8 Published online by Cambridge University Press

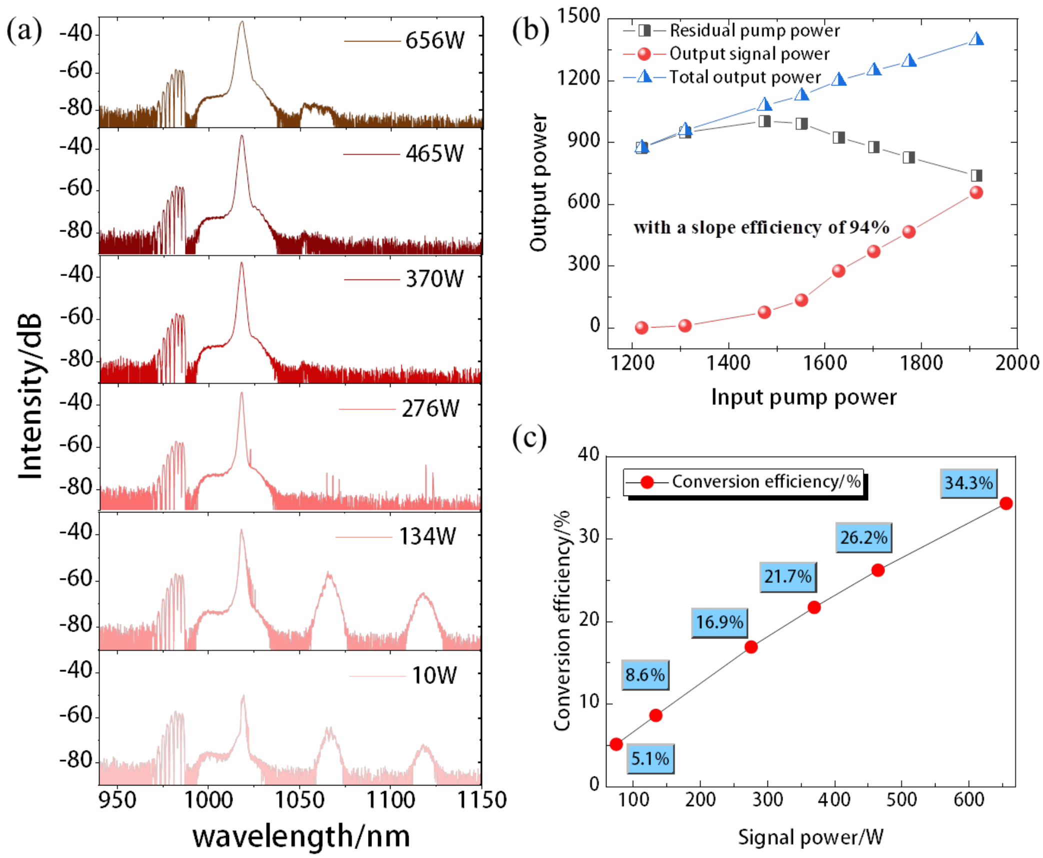

Figure 2. Output signal spectrum and power of RRFL (a) Output spectrum at different signal optical power levels; (b) Evolution characteristics of signal optical power with injected pump optical power. (c) The optical-to-optical conversion efficiency of signal light.

To gain a more visually intuitive understanding of the pump-signal light conversion relationship, a schematic diagram is presented in Figure 2(b). It can be observed that when the injected pump power reaches 1310W, the signal light begins to emit. Due to the half-open cavity structure of the random fiber laser, the weak random distributed feedback inside the fiber provides backward feedback, resulting in a higher emission threshold for the signal light compared to an oscillator. As the pump power exceeds 1310W, the power of the signal laser at 1018nm experiences a rapid increase. With further augmentation of the injected pump power, the pump energy swiftly converts into the signal light. At the maximum pump power of 1915W, the signal power reaches 656W, yielding a corresponding slope efficiency of 94%. The further increase in

https://doi.org/10.1017/hpl.2024.8 Published online by Cambridge University Press

power is limited by the combined effects of higher-order Raman and pump conversion efficiency. The suppression of higher-order Raman can be achieved by reducing the length of the fiber; however, this leads to an undesirable consequence of more residual pump light, significantly decreasing the pump's conversion efficiency. Hence, by balancing both higher-order Raman and pump conversion efficiencies, we achieved an output power of 656W.

The optical-to-optical (O-O) conversion efficiency of the laser system is the ratio of the signal light power to the input pump light power, while the electro-optical (EO) efficiency includes the power from the power supply to the fiber laser. The O-O conversion efficiency of the signal light is depicted in Figure 2(c). Through computation, it is revealed that as the injected pump power increases; the conversion efficiency of the signal light steadily improves, reaching a remarkable efficiency of 34.3% at the highest power level. Though there is too much residual pump power in the final output beam (more than 50 %)， and the total O-O conversion efficiency for this system is only 34.3%. However, the EO efficiency of this system can reach 20% [12]. This efficiency is comparable to that of a two-stage conversion (from LDs to YDFL, and then from YDFL to RRFLs).

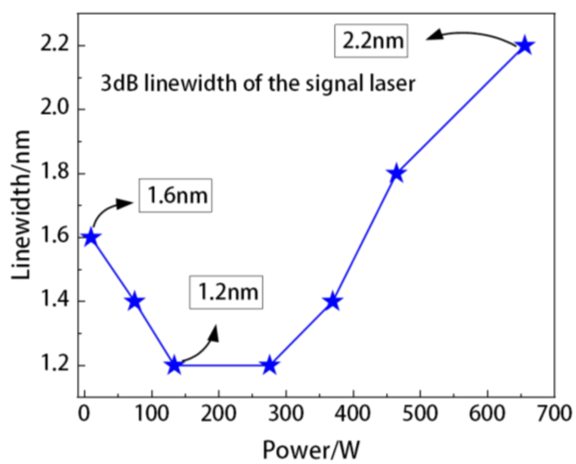

Figure 3. The output 3dB linewidth of signal laser at different output power levels.

https://doi.org/10.1017/hpl.2024.8 Published online by Cambridge University Press

Furthermore, we conducted an analysis of the changes in signal light linewidth as the signal power increases. In Figure 3, a distinct "notch" pattern can be observed in the signal light linewidth. Specifically, as the signal power increases, the linewidth initially decreases and then starts to increase. At an output power of 10W, the signal light linewidth measures at 1.6nm, and the minimum linewidth of around 1.2nm is achieved at a power of approximately 200W (this process corresponds to the gradual stabilization of the random fiber laser in the frequency domain, as depicted in Figure 2(a)). After the frequency domain stabilization of the random fiber laser, the signal light linewidth gradually increases with power, reaching a linewidth of 2.2nm at the highest power level.

Owing to the typical Schawlow–Townes spectral narrowing effect and the cascaded SBS effect of random distributed feedback fiber lasers near the lasing threshold [43], the RRFL pumped by LDs shows a relatively broad spectrum near the threshold. As the pump power increases, the cascaded SBS effect gradually diminishes, leading to the stabilization of the RRFL output temporal characteristics, resulting in a more stable output spectrum and a narrower linewidth of 1.2nm. Once the output temporal characteristics of the RRFL reach stability, with the continued increase in power from 280W to 656W, the influence of effects such as dispersion and mode coupling within the GRIN fiber causes a further broadening of the linewidth of the signal light. In reference [32], the spectral evolution characteristics of the RRFL, based on temporally stable ASE pump sources, also exhibit a phenomenon of initially narrowing and subsequently broadening.

B. The spatial domain characteristics of SW (1018nm) RRFL

Secondly, we conducted an investigation into the spatial characteristics of the RRFLs. Figure 4 illustrates the remarkable improvement in beam quality of the output signal light compared to the LDs pump source, with a beam quality factor of approximately 20. The left axis depicts the

https://doi.org/10.1017/hpl.2024.8 Published online by Cambridge University Press

beam quality of signal light at different power levels, while the right axis shows the corresponding BE. At a signal power around 100W, the beam quality measures at a commendable factor of 1.8. Although there is a slight degradation in beam quality with increasing power, reaching a factor of 2.9 at the highest output power, the BE continues to exhibit linear growth. At the peak power, the brightness is enhanced by a factor of 14.9. This is currently the highest known BE in RRFL structures. In the figure 4, we can also notice that, despite the continuous increase in brightness, the beam quality of the signal light is gradually deteriorating. This is primarily attributed to the rapid conversion of pump to Stokes within the fiber core, leading to the accumulation of heat [45]. Consequently, this heat accumulation gives rise to the thermal lens effect generated in the fiber core. Reference [45] investigated the thermal dissipation of a Raman fiber laser utilizing pure passive fiber as the gain medium. Through simulations of power distribution, the thermal characteristics of the Raman fiber laser, including the transverse and longitudinal distributions of heat load density, temperature, and thermally induced refractive index changes in the fiber were analyzed.

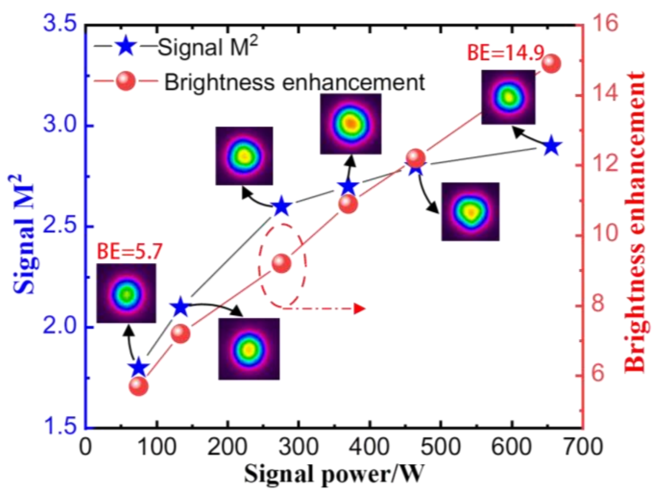

Figure 4. Beam quality factor M^2 (left axis) and the corresponding brightness enhancement (right axis) at different signal light power levels.

https://doi.org/10.1017/hpl.2024.8 Published online by Cambridge University Press

To further investigate the spatial characteristics of the pump light and the resulting Stokes signal laser in the RRFLs, we conducted measurements of the beam quality factors for both the pump light and the signal light, analyzing their evolution with respect to power. Figure 5 displays the measured data for the beam quality factors of the pump and the signal light at maximum power. A clear comparison reveals that the pump light's beam profile (as shown in Figure 5(a)) exhibits a speckle pattern, while the signal light's beam profile (as shown in Figure 5(b)) at the highest power level displays a Gaussian distribution. The insets within Figure 5 provide a visual representation of the near-field beam profile. The mechanisms underlying the BE have been extensively documented in various publications [46, 47]. Though the ability of GRIN fiber for power scaling and brightness enhancement has been proved in amplifier structure [48], the brightness of seed light plays a crucial role in the amplifier. In our work, the RRFL does not have seed light or a low-reflective grating with mode-selecting effects. Therefore, compared to previous work [13], this work is not only structurally innovative but also further verifies the brightness improvement and power scaling capabilities based on GRIN fibers.

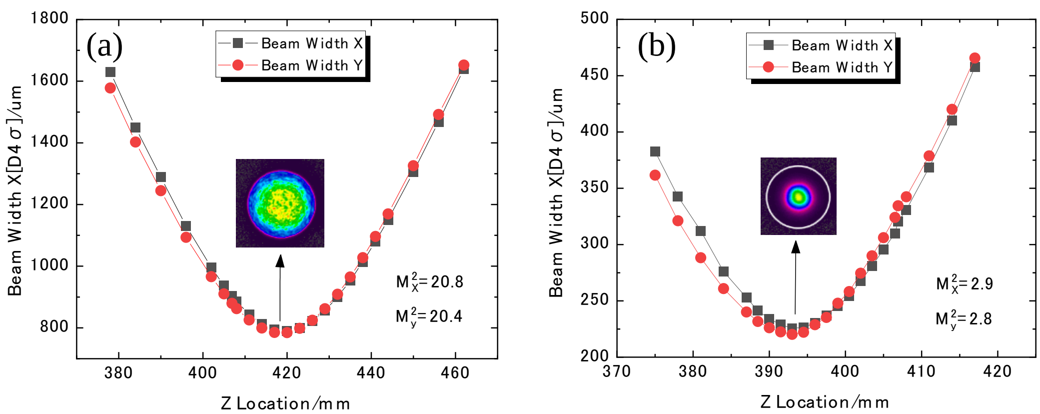

Figure 5. (a) Beam quality of pump Light; (b) Beam quality of signal light at maximum power.

https://doi.org/10.1017/hpl.2024.8 Published online by Cambridge University Press

Moreover, the utilization of graded-index (GRIN) fiber in random fiber lasers directly pumped by multimode LDs plays a vital role in enhancing the brightness. Due to the lower brightness of multimode LDs compared to YDFL, there are more higher-order modes present, leading to a more complex coupling process between different modes. By leveraging the Raman clean-up effect within GRIN fiber, unwanted higher-order modes can be effectively suppressed, resulting in improved beam quality [49]. In conclusion, the SW (1018nm) RRFL, which is pumped directly by LDs, demonstrates significant enhancement in the beam quality of the signal light, making it an ideal pump brightness converter in SWs output [50].

C. The temporal domain characteristics of SW (1018nm) RRFL

Thirdly, the temporal characteristics of the RRFL, which directly influence the observed unique spectral changes, are analyzed. Figure 6(a) displays the normalized time-domain measurement results of the RRFL signal output at different power levels over a 10ms time scale, utilizing an oscilloscope with a 1 GHz bandwidth. Since random fiber lasers lack a well-defined resonant cavity structure, their optical cavity dynamics are more intricate. During the initial stages of operation, the temporal stability of the random fiber laser experiences significant fluctuations. This phenomenon can also account for the presence of higher-order Raman peaks at 1070nm and 1120nm in Figure 2(a), even with a mere 10W of signal light power. The initial temporal instability results in the generation of intense pulse signals, facilitating the manifestation of higher-order SRS effects.

Due to the influence of cascaded SBS effects, the SBS factor can switch the quality factor (Q-value) of the RRFL and is present during the power escalation process [43]. Owing to the inherent stochastic nature of the SBS effect, unstable self-pulses with random intervals, durations, and amplitudes are observed. Furthermore, due to the impact of the SBS effect, the majority of

https://doi.org/10.1017/hpl.2024.8 Published online by Cambridge University Press

pulses have such weak intensities that they are nearly submerged beneath the noise baseline The first purely passive short-wavelength RFL directly pumped by multimode LDs was reported in [44], where the observation of unstable pulses with higher Stokes orders at a 1 W power level was also reported for the first time.

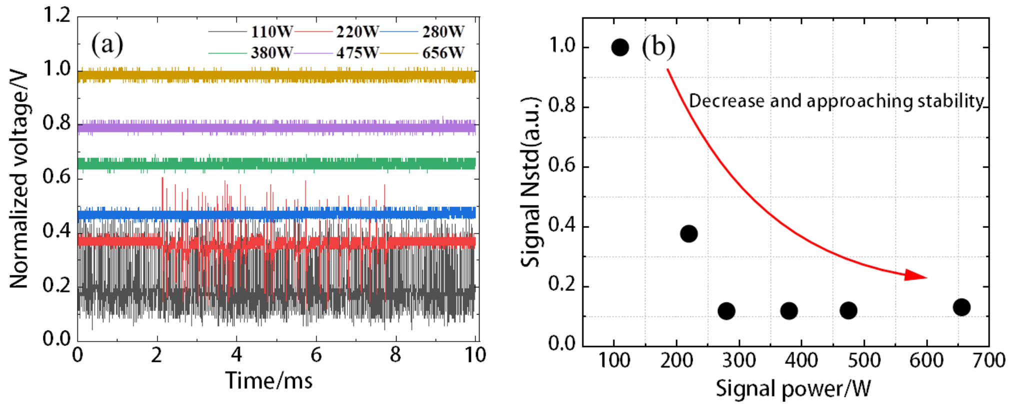

Figure 6. (a) The temporal stability characteristics of the RRFLs output signal light. (a) The normalized time domain measurement result of the RRFLs signal output at various power levels; (b) The normalized standard deviation (NSTD) of the output signal light intensity.

After the signal light power surpasses 280W, the temporal behavior of the random fiber laser gradually stabilizes, leading to an improvement in spectral purity and the disappearance of higher-order Raman spectrum. With further increase in pump power, the pump light energy swiftly converts into the signal light. Once the signal light intensity in the fiber reaches the threshold for second-order Raman scattering, the signal power starts transferring to higher-order Raman frequency shift, resulting in a rapid amplification of the second-order Raman spectrum. Figure 6(b) illustrates the referenced normalized standard deviation (NSTD) of the output intensity. This NSTD decreases as the power is scaled up to higher levels, indicating a progressive improvement in the temporal stability of the signal laser. Although there have been reports discussing the temporal fluctuations [42], the precise dynamics underlying these processes remain somewhat unclear and necessitate further analysis by researchers.

The dynamics of intensity fluctuation transfer is an area of research that has seen progress in RRFLs. Understanding and controlling the intensity fluctuations in RRFLs are crucial for optimizing their performance and stability. Researchers have studied and developed techniques to manage and mitigate intensity fluctuations, thereby improving the performance and reliability of lasers. Furthermore, the RDFB mechanism introduces mode-free characteristics and distinctive statistical properties, making RRFLs fascinating and excellent platforms for scientific research and practical applications [31]. In a RRFL, it's important to note that multiple longitudinal modes can be generated and compete for gain within the laser cavity. This mode competition gives rise to irregular intensity fluctuations and rapid variations in output power over time.

IV. CONCLUSION

In conclusion, we demonstrate an all-fiberized, purely passive short-wavelength RRFL directly pumped by multimode LDs. The power record of purely passive RRFL excluding any active dopant in the whole system is obtained to 656 W at 1018 nm. To the best of our knowledge, this achievement also represents the highest power record of RRFL utilizing multimode LDs for direct pumping at the wavelength. The slope efficiency is 94% and electro-optical conversion efficiency is ~20%. The beam quality M^2 factor is 2.9 (which is ~20 of pump) at the maximum output signal power, achieving the highest brightness enhancement (BE) of 14.9 in RRFLs. The work could not only pave the way for achieving high-power SWs laser output through multimode LDs direct pumping of passive fibers, but also providing a new insight into the realization of high-power, high-brightness RRFLs below 1 μm .

Acknowledgement

https://doi.org/10.1017/hpl.2024.8 Published online by Cambridge University Press

This work is supported by National Natural Science Foundation of China (62061136013, 12174445). The authors thank Prof. Zilun Chen for providing the fiber end cap; thank Mr. Liang Xiao for technical supporting in the experiment.

References

1. Logan G. Wright, Fan O. Wu3, Demetrios N. Christodoulides3, null, Frank W. Wise1. Physics of highly multimode nonlinear optical systems. Nat. Phys. 18, 1018 (2022). Doi: 10.1038/s41567-022-01691-z.
2. Pu Zhou, Hu Xiao, Jinyong Leng, Jiangming Xu, Zilun Chen, Hanwei Zhang, and Zejin Liu. High-power fiber lasers based on tandem pumping. J. Opt. Soc. Am.B 34, A29(2017). Doi: 10.1364/JOSAB.34.000A29.
3. Zervas, Michalis N.; Codemard, Christophe A. High power fiber lasers: A review. IEEE J. Sel. Top. Quant. Electron. 20, 219 (2014). Dio: 10.1109/JSTQE.2014.2321279.
4. Min Jiang, Hanshuo Wu, Yi An, Tianyue Hou, Qi Chang, Liangjin Huang, Jun Li, Rongtao Su, and Pu Zhou. Fiber laser development enabled by machine learning: review and prospect. PhotoniX 3, 1 (2022). Doi: 10.1186/s43074-022-00055-3.
5. Cesar Jauregui, Christoph Stihler, and Jens Limpert. Transverse mode instability. Adv. Opt. Photonics 12, 429 (2020). Doi: 10.1364/AOP.385184.
6. Liang Dong. Transverse Mode Instability in Raman Fiber Amplifiers. IEEE J. Quant. Electron. 59, 1 (2023). Doi: 10.1109/JQE.2023.3253183.
7. Shadi Naderi, Iyad Dajani, Jacob Grosek, Timothy Madden. Theoretical and numerical treatment of modal instability in high-power core and cladding pumped Raman fiber amplifiers. Opt. Express 24, 16550 (2016). Doi: 10.1364/OE.24.016550.
8. Jun Ye, Jiangming Xu, Jiaxin Song, Yang Zhang, Hanwei Zhang, Hu Xiao, Jingyong Leng, and Pu Zhou, Pump scheme optimization of an incoherently pumped high-power random fiber laser. Photon. Res. 7, 977 (2019). Doi: 10.1364/PRJ.7.000977.
9. Qiuhui Chu, Pengfei Zhao, Honghuan Lin, Yu Liu, Chengyu Li, Bopeng Wang, Chao Guo, Xuan Tang, Chuangxiang Tang, and Feng Jing. kW-level 1030 nm polarization-maintained fiber laser with narrow linewidth and near-diffraction-limited beam quality. Appl. Opt. 57, 2992 (2018). Doi: 10.1364/AO.57.002992.

https://doi.org/10.1017/hpl.2024.8 Published online by Cambridge University Press

10. Bo Cao, Chenxin Gao, Yihang Ding, Xiaosheng Xiao, Changxi Yang, Chengying Bao. Self-starting spatiotemporal mode-locking using Mamyshev regenerators. Opt.Lett. 47, 4584 (2022). Doi: 10.1364/OL.469291.
11. Pei Ju, Wenhui Fan, Baoyin Zhao, Wei Gao, Tongyi Zhang, Gang Li, Qi Gao, and Zhe Li, High power, tunable, ultra-narrowband Yb-doped superfluorescent fiber source operating at wavelength less than 1055 nm with 20 nm tuning range. Infrared Phys. Technol. 111, 103530 (2020). Doi: 10.1016/j.infrared.2020.103530.
12. Chenchen Fan, Yizhu Chen, Tianfu Yao, Hu Xiao, Jiangming Xu, Jinyong Leng, Pu Zhou, Alexey A. Wolf, Ilya N. Nemov, Alexey G. Kuznetsov, Sergey I. Kablukov, and Sergey A. Babin. Over 400 W graded-index fiber Raman laser with brightness enhancement. Opt. Express 29, 19441 (2021). Doi: 10.1364/OE.427605.
13. Chenchen. Fan, Yi An, Yang Li, Xiulu Hao, Tianfu Yao, Hu Xiao, Liangjin Huang, Jiangming Xu, Jinyong Leng, and Pu Zhou. Modal Dynamics in Kilowatt Cladding-Pumped Random Distributed Feedback Raman Fiber Laser With Brightness Enhancement. J. Lightwave Technol. 40, 19 (2022). Doi: 10.1109/JLT.2022.3194534.
14. Sergey A. Babin. High-brightness all-fiber Raman lasers directly pumped by multimode laser diodes. High Power Laser Sci. Eng. 7, e15 (2019). Doi: 10.1017/hpl.2018.76.
15. Ruixian Li, Haobo Li, Hanshuo Wu, Hu Xiao, Jinyong Leng, Liangjin Huang, Zhiyong Pan, Pu Zhou. Mitigation of TMI in an 8 kW tandem pumped fiber amplifier enabled by inter-mode gain competition mechanism through bending control. Opt. Express 31, 24423 (2023). Doi: 10.1364/OE.486915.
16. Zhaoxin Xie, Qiang Fang, Yang Xu, Xuelong Cui, Quan Sheng , Wei Shi, and Jianquan Yao. Hundred-watts-level monolithic narrow linewidth linearly-polarized fiber laser at 1018 nm. Opt. Eng., 58, 106106 (2019). Doi: 10.1117/1.OE.58.10.106106.
17. Palma-Vega, Gonzalo, Walbaum, Till, Heinzig, Matthias, Kuhn, Stefan, Hupel, Christian, Hein, Sigrun, Feldkamp, Gerrit, Sattler, Bettina, Nold, Johannes, Haarlammert, Nicoletta, Schreiber, Thomas, Eberhardt, Ramona, Tuennermann, Andreas. Ring-up-doped fiber for the generation of more than 600 W single-mode narrow-band output at 1018 nm. Opt. Lett. 44, 2502 (2019). Doi: 10.1364/OL.44.002502.
18. Kang-Jie Lim, Samuel Kal-Wen Seah, Joash Yongen Ye, Wengy Weiying Lim, Chu-Perng Seah, Yunn-Boon Tan, Suting Tan, Huiting Lim, Raghuraman Sidharthan,

https://doi.org/10.1017/hpl.2024.8 Published online by Cambridge University Press

Arumugam Rajendar. Prasadh, Chen-Jian Chang, Seongwoo Yoo, and Song-Liang Chua. High absorption large-mode area step-index fiber for tandem-pumped high-brightness high-power lasers. Photon. Res. 8, 1599 (2020). Doi: 10.1364/PRJ.400755.

19. Yaakov Glick, Yoav Sintov, Roey Zuitlin, Shaul Pearl, Yariv Shamir, Revital Feldman, Zvi Horvitz, and Noam Shafir. Single-mode 230 W output power 1018 nm fiber laser and ASE competition suppression. J. Opt. Soc. Am.B. 33, 1392(2016). Doi: 10.1364/JOSAB.33.001392.
20. Christoph Ottenhues/Ottenhues C, Thomas Theeg/Theeg T, Katharina Hausmann/Hausmann K, Mateusz Wysmolek/Wysmolek M, Hakan Sayinc/Sayinc H, Jörg Neumann/Neumann J, Dietmar Kracht/Kracht D. Single-mode monolithic fiber laser with 200 W output power at a wavelength of 1018 nm. Opt. Lett. 40, 4851 (2015). Doi: 10.1364/OL.40.004851.
21. Jianhua Wang, Gui Chen, Lei Zhang, Jinming Hu, Jinyan Li, Bing He, Jinbao Chen, Xijia Gu, Jun Zhou, and Yan Feng. High-efficiency fiber laser at 1018 nm using Yb-doped phosphosilicate fiber. Appl. Opt. 51, 7130–7133 (2012). Doi: 10.1364/AO.51.007130.
22. Chu Perng Seah, Tze Yang Ng, and Song-Liang Chua. 400W Ytterbium-doped fiber oscillator at 1018nm. In Advanced Solid State Lasers Conference, paper ATu2A.33 (2015).
23. Ping Yan, Xuehao Wang, Zehui Wang, Yusheng Huang, Dan Li, Qirong Xiao, and Mali Gong. A 1150 W 1018 nm fiber laser bidirectional pumped by wavelength-stabilized laser diodes. IEEE J. Sel. Top. Quant. Electron. 24, 1 (2018). Doi: 10.1109/JSTQE.2018.2805801.
24. Salih K Kalyoncu; Aydın Yeniay. High Brightness 1018 Nm Monolithic Fiber Laser With Power Scaling to >500 W. Appl. Opt., 59, 4763 (2020). Doi: 10.1364/AO.393043.
25. Nikolai Platonov;Oleg Shkurikhin;Valentin Fomin;Daniil Myasnikov;Roman Yagodkin;Anton Ferin;Alexey Doronkin;Ivan Ulyanov;Valentin Gapontsev. High-efficient kW-level single-mode ytterbium fiber lasers in all-fiber format with diffraction-limited beam at wavelengths in 1000-1030 nm spectral range. Fiber Lasers XVII: Technology and Systems (2020).
26. P. Wang, J. K. Sahu, and W. A. Clarkson. Efficient single-mode operation of a cladding-pumped ytterbium-doped helical-core fiber laser. Opt. Lett. 31, 3116(2006). Doi: 10.1364/OL.31.000226.

27. Jiangming Xu, Jun Ye, Wei Liu, Jian Wu, Hanwei Zhang, Jinyong Leng, and Pu Zhou, Near-diffraction-limited linearly polarized narrow-linewidth random fiber laser with record kilowatt output. Photon. Res. 5, 598 (2017). Doi: 10.1364/PRJ.5.000350.
28. Knall, Jennifer M., Engholm Magnus, Boilard Tommy, Bernier Martin, Vigneron Pierre Baptiste, Yu Nanjie, Dragic Peter D., Ballato John M., Digonnet, Michel J.F. Radiation-balanced silica fiber laser. Optica 8, 830 (2021). Doi: 10.1364/OPTICA.425115.
29. Yu, N., Cavillon, M., Kucera, C., Hawkins, T.W., Ballato, J., Dragic, P. Less than 1% quantum defect fiber lasers via ytterbium-doped multicomponent fluorosilicate optical fiber. Opt. Lett. 43, 3096 (2018). Doi: 10.1364/OL.43.003096.
30. Sergei K. Turitsyn, Sergey A. Babin, Atalla E. El-Taher, Paul Harper, Dmitriy V. Churkin, Sergey I. Kablukov, Juan Diego Ania-Castañón, Vassilis Karalekas, Evgenii V. Podivilov. Random distributed feedback fibre laser. Nat. Photonics 4, 231 (2010). Doi: 10.1038/nphoton.2010.4.
31. Sergei K. Turitsyn, Sergey A. Babin, Dmitry V. Churkina, Ilya D. Vatnik, Maxim Nikulin, Evgenii V. Podivilov. Random distributed feedback fibre lasers(Review). Phys. Rep. 542, 133 (2014). Doi: 10.1016/j.physrep.2014.02.011.
32. Jun Ye, Xiaoya Ma, Yang Zhang, Jiangming Xu, Hanwei Zhang, Tianfu Yao, Jinyong Leng, and Pu Zhou. Revealing the dynamics of intensity fluctuation transfer in a random Raman fiber laser. Photon. Res. 10, 619 (2022). Doi: 10.1364/PRJ.445432.
33. Ekaterina A. Evmenova, Alexey G. Kuznetsov, Ilya N. Nemov, Alexey A. Wolf, Alexandr V. Dostovalov, Sergey I. Kablukov, Sergey A. Babin. 2nd-order random lasing in a multimode diode-pumped gradedindex fiber. Sci. Rep. 8, 17495 (2018). Doi: 10.1038/s41598-018-35767-9.
34. Ruixian Li, Hanshuo Wu, Hu. Xiao, Jinyong Leng, and Pu Zhou. More than 5 kW counter tandem pumped fiber amplifier with near single-mode beam quality. Opt. Laser Technol. 153, 108204 (2022). Doi: 10.1016/j.optlastec.2022.108204.
35. Hanshuo Wu, Ruixian Li, Hu Xiao, Jinyong Leng, and Pu Zhou. Comprehensive investigations on the tandem pumping scheme employing the pump fiber laser operating at an extremely short wavelength. Opt. Express 29, 34880 (2021). Doi: 10.1364/OE.434218.
36. Xiaoya Ma, Jiangming Xu, Jun Ye, Yang Zhang, Liangjin Huang, Tianfu Yao, Jinyong Leng, Zhiyong Pan, Pu Zhou. Cladding-pumped Raman fiber laser with 0.78% quantum

defect enabled by phosphorus-doped fiber. High Power Laser Sci. Eng. 10, 5 (2022). Doi: 10.1017/hpl.2021.60.

37. Zlobina, E.A., Kablukov, S.I., Wolf, A.A., Dostovalov, A.V., Babin, S.A.. Nearly single-mode Raman lasing at 954 nm in a graded-index fiber directly pumped by a multimode laser diode. Opt. Lett. 42, 9 (2017). Doi: 10.1364/OL.42.000009.
38. Yaakov Glick; Viktor Fromzel; Jun Zhang; Nikolay Ter-Gabrielyan; Mark Dubinskii. High-efficiency, 154 W CW, diode-pumped Raman fiber laser with brightness enhancement. Appl. Opt. 56, B97 (2017). Doi: 10.1364/AO.56.000B97.
39. Alexey G. Kuznetsov, Sergey I. Kablukov, Evgeny V. Podivilov, and Sergey A. Babin. Brightness enhancement and beam profiles in an LD-pumped graded-index fiber Raman laser. OSA Continuum. 4, 1034 (2021). Doi: 10.1364/OSAC.421985.
40. Soonki Hong; Yutong Feng; Johan Nilsson. Off-Peak Dual-Wavelength Multimode Diode-Laser- Pumped Fiber Raman Laser. IEEE photo. Technol. Lett. 30, 1625 (2018). Doi: 10.1109/LPT.2018.2863559.
41. Soonki Hong; Yutong Feng; Johan Nilsson. Wide-Span Multi-Wavelength High-Power Diode-Laser Pumping of Fiber Raman Laser. IEEE photo. Technol. Lett. 31, 1995 (2019). Doi: 10.1109/LPT.2019.2953195.
42. Jun Ye, Xiaoya Ma, Yang Zhang, Jiangming Xu, Hanwei Zhang, Tianfu Yao, Jinyong Leng, and Pu Zhou. From spectral broadening to recompression: dynamics of incoherent optical waves propagating in the fiber. PhotoniX 2, 15 (2021). Doi: 10.1186/s43074-021-00037-x.
43. Jiangming Xu, Jian Wu, Jun Ye, Jiaxin Song, Baicheng Yao, Hanwei Zhang, Jinyong Leng, Weili Zhang, Pu Zhou, and Yunjiang Rao. Optical rogue wave in random fiber laser. Photon. Res. 8, 1(2020). Doi: 10.1364/PRJ.8.000001.
44. Babin, S.A., Dontsova, E.I., Kablukov, S.I. Random fiber laser directly pumped by a high-power laser diode. Opt. Lett. 38, 3301 (2013). Doi: 10.1364/OL.38.003301.
45. Yizhu Chen, Tianfu Yao, Hu Xiao, Jinyong Leng, Pu Zhou. Theoretical analysis of heat distribution in Raman fiber lasers and amplifiers employing pure passive fiber. IEEE photonics journal , 12, 1 (2020). Doi: 10.1109/JPHOT.2020.3038350.

46. Yizhu Chen, Tianfu Yao, Hu Xiao, Jinyong Leng, and Pu Zhou. Greater than 2kW all-passive fiber Raman amplifier with good beam quality. High Power Laser Sci. Eng. 8, e33 (2020). Doi: 10.1017/hpl.2020.33.
47. Oleg S Sidelnikov, Evgeny V Podivilov, Mikhail P Fedoruk, Alexey G Kuznetsov, Stefan Wabnitz, Sergey A Babin. Mechanism of brightness enhancement in multimode LD-pumped graded-index fiber Raman lasers: numerical modeling .Opt. Express 30, 8212 (2022). Doi: 10.1364/OE.449773.
48. Yizhu Chen, Tianfu Yao, Hu Xiao, Jinyong Leng, and Pu Zhou. 3 kW Passive-Gain-Enabled Metalized Raman Fiber Amplifier With Brightness Enhancement. J. Lightwave Technol. 39, 1785 (2021). Doi: 10.1109/JLT.2020.3039677.
49. Supradeepa, V. R., Feng Yan, Nicholson, Jeffrey W. Raman fiber lasers. J. Opt. 19, 023001 (2017). Doi: 10.1088/2040-8986/19/2/023001.
50. Govind P. Agrawal. Spatial beam narrowing in Raman amplifiers made with graded-index multimode fibers: a semi-analytic approach. J. Opt. Soc. Am.B 40, 715 (2023). Doi: 10.1364/JOSAB.482730.